Study of the risk of damage to buried networks and equipment during vegetation fires

Idir KHALDI[1*], Lucas TERREI[1], Anthony COLLIN[1]

[1]Université de Lorraine, CNRS, LEMTA, Nancy, F-54000, France
*(Corresponding author: idir.khaldi@univ-lorraine.fr)

Abstract - Wildland fires impose thermal loads that can affect the subsurface, including thermoplastic networks (PVC/HDPE) and locally, historical munitions. The objective is to assess heat propagation in soil exposed to radiative heat fluxes representative of a flame front and to estimate the depths at which critical thresholds are reached: 60 °C for networks and 120 °C for munitions. Two complementary experimental campaigns were carried out to measure the heat flux densities received at ground level and then to measure thermal diffusion with depth. The results show that these thresholds can be exceeded within the first centimeters of soil. In the most severe case (50 kW.m^{-2}), the 120 °C threshold is reached down to a depth of 3 cm.

1. Introduction

Wildfires represent a growing threat to many countries around the world and particularly in France [1]. Their intensification is directly linked to climate change and actively contributes to the increase in the greenhouse effect [2]. This phenomenon is becoming all the more alarming as it now affects the wildland-urban interface. Significant issues also lie in the subsoil of land exposed to these fires. Many underground infrastructures are made of polyvinyl chloride (PVC) and/or high-density polyethylene (HDPE), whose critical operating threshold is 60 °C. Any damage could have significant repercussions for the safety of residents and the continuity of public services. Furthermore, certain regions of France were heavily exposed to the last two world wars. There are still more than 350 million war munitions buried in the ground, which can pose a mortal danger to people. A temperature of 120 °C is considered a critical threshold for these munitions. Despite their burial, the risks remain significant, as intense heatwaves can spread through the ground and trigger the munitions. Regarding depth, estimates vary: small munitions are between 10 and 30 cm deep, while bombs can be buried between 2 and 10 m deep, according to the Directorate of Memory, Culture and Archives. However, this burial is not permanent. Under the combined action of freeze/thaw cycles (cryoturbation) and the "Brazil nut" effect (upward migration by granular segregation), these munitions undergo a slow vertical migration that inexorably pushes them to resurface over time.

Much experimental work has been devoted to the study of the thermal conditions that can be generated by a wildfire. The main measurements are temperatures and received heat fluxes, but these are often related to the flame front propagation rather than to ground level. For instance, Silvani and Morandini have highlighted heat fluxes ranging from 25 to 51 kW·m^{-2} (radiative) and from 40 to 112 kW·m^{-2} (total), depending on the type of vegetation [3]. Frankman *et al.* showed that the maximum values of radiative fluxes depend on the type of fire: 18 to 115 kW·m^{-2} for surface fires, up to 132 kW·m^{-2} for brush fires and up to 300 kW·m^{-2} for crown fires [4]. Residence times generally range from 10 to 40 seconds, but often exceed 40 seconds in the case of brush fires. For comparison, Mueller *et al.* reported that surface fires reached 32 kW·m^{-2}, while crown fires were measured at a maximum of 52 kW·m^{-2} [5]. Radiation is the dominant mode of transfer in the preheating zone, whereas convection becomes

https://doi.org/10.25855/SFT2026-084

more significant in the combustion zone. The authors emphasize the importance of correcting for uncertainties in the measurement method when characterizing wildfire intensity and scale.

Other research focuses particularly on the thermal constraints imposed by fire and the mechanisms of heat propagation in the ground. Busse *et al.* investigated soil heating during the burning of slash and wood piles and K-type thermocouples were placed at different depths in the soil [6]. The results showed that wood piles generate temperatures reaching 225–314 °C at 5–10 cm depth, with a heating time of over 20 h. Conversely, slash piles generally do not exceed 200 °C at 5 cm and 100 °C at 10 cm, which limits their effect on the soil. The study concludes that the pile size is not a reliable indicator of the risk of extreme heating, but it is mainly the proportion of large wood that determines the thermal impact. Richter numerically studied heat transfers in the ground and their impact on PVC and HDPE pipes with a maximum operating temperature of 60 °C [7]. The results showed that burial depth was the most determining factor. Thus, for a surface temperature of 600 °C maintained for 4 h, the threshold of 60 °C was reached up to 0.41 m depth; and for 900 °C over the same duration, up to 0.45 m, close to the recommended depth of 0.46 m. Janssens developed a calculation method to predict temperature profiles in soil exposed to the heat of a forest fire and to assess its effect on buried thermoplastic pipes [8]. The aim was to determine the probability that a fire would raise the surface temperature of a pipe buried 0.3 m deep above 60 °C. The method highlights the significant impact of considering water evaporation. While Richter estimated the probability of exceeding 60 °C at a depth of 0.3 m at 17% [7]. Janssens shows on the contrary that this probability becomes zero, even for intense and prolonged fires [8]. Rein *et al.* investigated the effects of peatland smouldering on forest soils [9]. Laboratory experiments were conducted on boreal peat samples ($100 \times 100 \times 50$ mm^3) subjected to an external ignition source, with temperature monitoring. The results showed that humidity controls ignition and temperature reaching 500–600 °C for over 20 minutes in some cases. These conditions are sufficient to sterilize the soil and cause irreversible transformations.

The literature shows that vegetation fires generate intense thermal stresses that can alter the thermal dynamics of soils. However, the available results exhibit considerable variability, stemming from differences in methodology, experimental conditions and studied parameters (heat flux and exposure duration). New experimental investigations are therefore required to complement existing data and more accurately represent real fire conditions, by characterizing both the surface thermal load and the heat diffusion in depth.

2. Materials and Methods

2.1. Characterization of the heat flux densities received by the soil

The first experimental campaign is based on the use of a steel burn table (Figure 1) measuring 1.5×1.2 m^2, equipped with a metal mesh composed of square cells of 5 cm per side to ensure a homogeneous distribution of the fuel. The fuel used is wood shavings, whose characteristics (Table 1) are taken from the work of Marchand [10]. The wood shavings are kept in a closed and insulated storage room to limit significant variations in moisture and temperature. Based on the work of Laverdière and Thibaudeau, three fuel loads were selected for this study: 0.175, 0.575 and 0.875 kg.m^{-2} [11]. These values correspond respectively to a field with stubble, a field with crop residues and a field with standing crop. A total heat flux meter, cooled by water and placed in the center of the table, allows measuring the heat flux densities received at ground level. This central positioning avoids lateral heat losses. Since the flame front forms a U-shape, the heat flux meter captures the maximum thermal intensity there, which is representative of the core of the fire. It is supplied by the Captec company and is based on the Seebeck effect. The heat flux meter is calibrated with a black body. In parallel, type K thermocouples with a diameter of 0.15 mm are placed every 20 cm along the table. They make it possible to evaluate the rate of spread of the flame front as well as the residence time. Each load was tested three times to ensure repeatability. Ignition is carried out using a blowtorch, moving across the wood shaving bed from one end to the other in order to create a regular flame front.

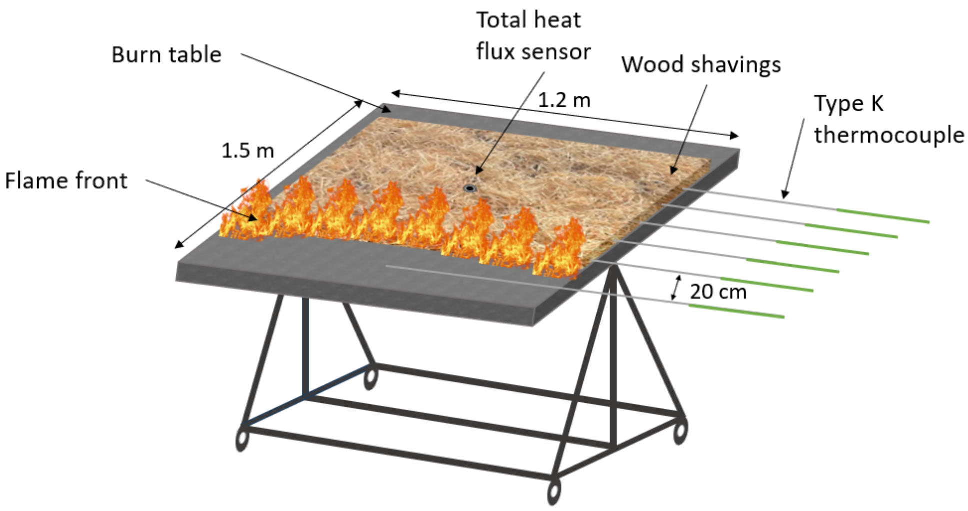

Figure 1: Schematic of the experimental setup on theburning table.

Table 1: Mean characteristics of the wood shavings.

Length (mm)	Width (mm)	Thickness (mm)	Density (kg.m^{-3})	Moisture (%)
89.1	1.96	0.16	519	12

2.2. Characterization of critical depths

The second experimental campaign aims to analyze thermal propagation in depth under controlled radiative fluxes. In order to ensure the repeatability of the tests, each heat flux density is tested three times. The precise control of the imposed heat flux densities is achieved using a propane-fueled radiant panel measuring 50 $\times$ 50 cm^2. The imposed heat flux was determined by a prior calibration, linking the panel-to-soil distance to the heat flux measured by a heat flux meter. The surface area of the panel (50 $\times$ 50 cm^2) is smaller than that of the tank (64 $\times$ 64 cm^2). The distribution of the radiation is therefore heterogeneous on the surface, but the in-depth temperature measurement is performed in the center, at the location of the incident heat flux measurement. It is therefore considered that this measurement is relatively unaffected by edge effects. An exposure duration of 12 minutes was adopted, which is consistent with the average residence times observed in the field for fires at a single location and the operational safety margins of firefighters. The setup (Figure 2) consists of a steel tank measuring 64 $\times$ 64 $\times$ 58 cm^3 filled with dry sand (0.04% moisture), selected because it represents an inert material. This sand has a density of $\rho = 2650$ kg.m^{-3} and an effective thermal conductivity of $\lambda = 0.245$ W.m^{-1}.K^{-1}. The instrumentation consists of ten K-type thermocouples with a diameter of 0.15 mm, inserted every centimeter down to a depth of 10 cm through a perforated lateral structure.

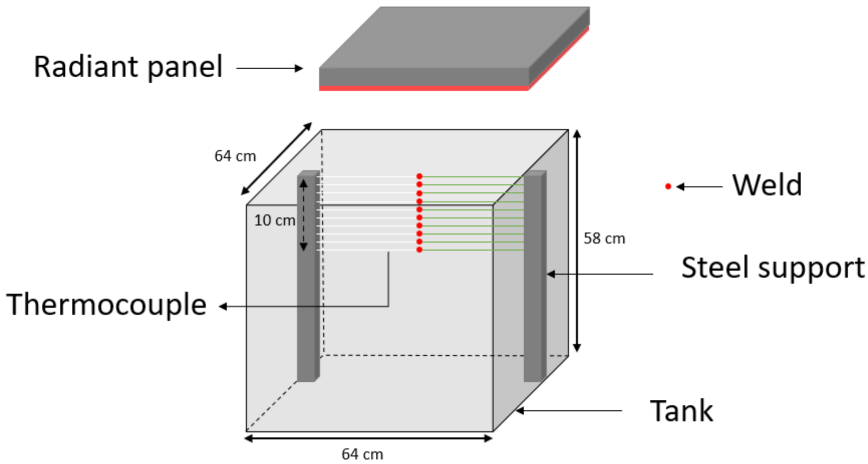

Figure 2: Schematic of the experimental setup.

To account for the variations in initial conditions related to the cooling of the tank (1 h 48), the results are analyzed using the temperature variation:

$$\Delta T(x,t) = T(x,t) - T(x,0) \tag{1}$$

where $T(x,t)$ corresponds to the temperature measured at depth x and time t and $T(x,0)$ to the initial temperature at the same depth.

3. Results

3.1. Heat flux densities, rate of spread and residence time

The mean values of the measured heat flux densities φ, rates of spread ROS and residence times t_r are presented in Table 2.

Table 2: Summary of the measurements on the burn table (mean ± standard deviation).

Load	ROS	t_r	φ
(g.m^{-2})	(cm.s^{-1})	(s)	(kW.m^{-2})
175	1.03 ± 0.10	80 ± 6	20.95 ± 2.14
575	1.66 ± 0.10	54 ± 7	39.82 ± 3.44
875	1.34 ± 0.10	78 ± 4	45.24 ± 13.65

The rate of spread (ROS) increases with the fuel load, going from 1.03 cm.s^{-1} for 175 g.m^{-2} up to a plateau of 1.66 cm.s^{-1} for 575 g.m^{-2} and then slightly decreases as the load continues to grow to 1.34 cm.s^{-1} for 875 g.m^{-2}. This behavior can be explained by the physics of fire propagation. At low fuel loads, the amount of available material is limited, the flame front releases little energy and heat transfer to the unburned fuel remains modest, which slows down propagation. As the fuel load increases, the energy released by combustion also rises, the flames become taller and more radiant, promoting rapid heating of the fuel ahead of the front and thus accelerating the rate of spread. However, beyond a certain threshold, the thickness of the fuel bed becomes too great, oxygen supply is limited in depth, combustion becomes heterogeneous and the flame tends to develop vertically rather than horizontally. This non-linear evolution is consistent with the findings of Rothermel [12].

The obtained residence times (duration during which the studied surface is exposed to the flame front) are approximately one minute. These orders of magnitude are consistent with the residence times reported in the literature for vegetation fires, notably by [4, 5].

A clear increase in received heat flux density is observed between 175 g.m^{-2} and 575 g.m^{-2}, while at the highest load (875 g.m^{-2}), the flux density tends to plateau around 45 kW.m^{-2}. This saturation can be explained by an imbalance between the available fuel mass and the combustion conditions. Thus, increasing the fuel load globally enhances the released heat flux density, but only up to a certain threshold beyond which combustion becomes less efficient. Table 2 highlights a higher standard deviation for the 875 g.m^{-2} load. This variability reflects a heterogeneous combustion due to this configuration: the significant thickness of the wood shaving bed (approximately 20 cm) limits the oxygen supply in the lower layers and generates tall flames, causing strong fluctuations in thermal radiation. The maximum value obtained ($\sim$ 50 kW.m^{-2}) lies within the range reported in the literature for surface vegetation fires, which supports the relevance of the experiments [3, 4]. The uncertainty due to the aging of the heat flux meter was taken into account by checking the sensor's calibration after each test, thereby ensuring that no alteration of its initial calibration falsifies the measurements.

These results lead to the selection of three representative heat flux density levels for the remainder of the study: 20 kW.m^{-2}, 40 kW.m^{-2} and 50 kW.m^{-2}. These values correspond to realistic and adverse scenarios for buried networks and will serve as the basis for the thermal propagation experiments in the soil.

3.2. Temperature in the soil

Figures 3 and 4 show the in-depth temperatures according to the applied heat flux. The red line indicates the point at which the radiant panel is turned off and the two dashed lines the criteria at 60 °C and 120 °C.

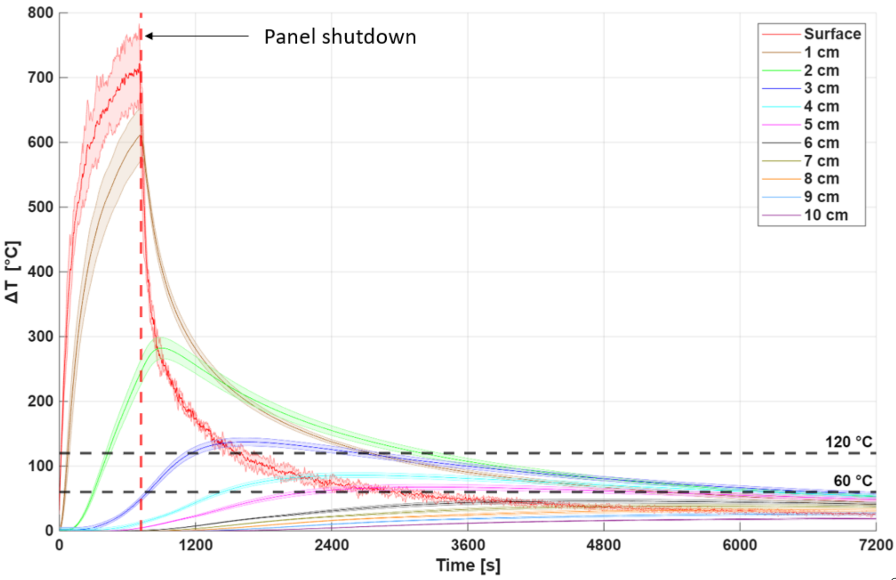

Figure 3: Temporal evolution of ΔT according to depth for 50 kW.m^{-2}.

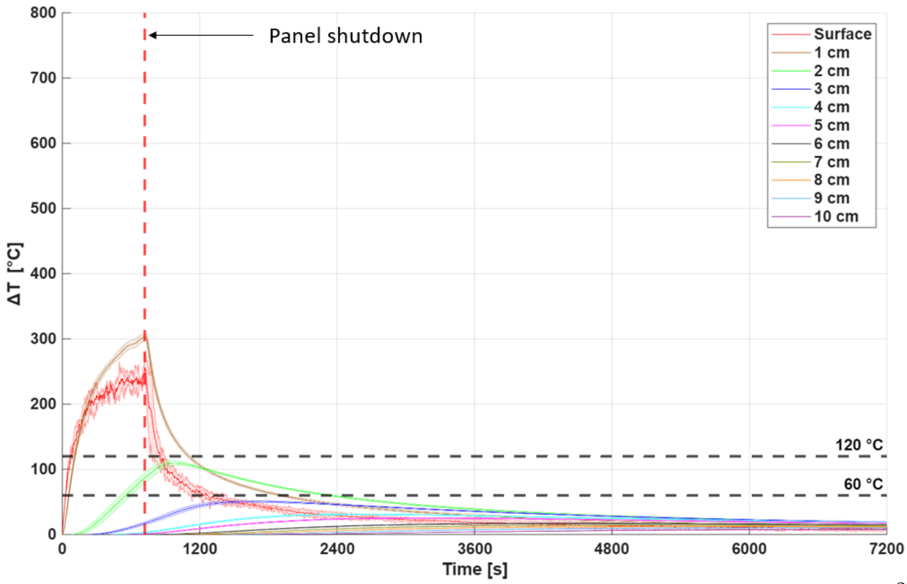

Figure 4: Temporal evolution of ΔT according to depth for 20 kW.m^{-2}.

At 50 kW.m^{-2}, the surface temperature rises very rapidly during the heating phase, reaching an average maximum of 722 °C. Heating is particularly pronounced in the first two centimeters of soil, then the attenuation becomes noticeable with depth. The critical threshold of 60 °C is exceeded only in the first five centimeters, while the threshold of 120 °C is only reached in the first three centimeters. Once the panel is no longer powered, the surface cools immediately, while the deeper layers continue to heat up by conduction. The 60 °C threshold is exceeded at a depth of 1 to 3 cm until the end of the test, while the 120 °C threshold remains exceeded for approximately 40 minutes after shutdown in the same area. After two hours of testing, the ground temperature stabilizes between 20 °C (at 10 cm) and 60 °C (at 3 cm) depending on the depth.

For 20 kW.m^{-2}, the maximum surface temperature is approximately 256 °C, while at a depth of 1 cm it rises to 298 °C, reflecting heat storage. This phenomenon is due to the fact that the surface cools faster through convection, while heat remains trapped at depth. The critical threshold of 60 °C is only exceeded in the first two centimeters, while the threshold of 120 °C is only exceeded in the very first centimeter. When the panel's power supply is interrupted, the surface and the 1 cm layer cool down immediately, while heat continues to diffuse to the deeper layers. The 60 °C threshold is exceeded for around thirty minutes after shutdown, while the 120 °C threshold is only exceeded for about ten minutes. After two hours of testing, the ground temperature stabilizes between 18 °C at a depth of 3 cm and 8 °C at a depth of 10 cm.

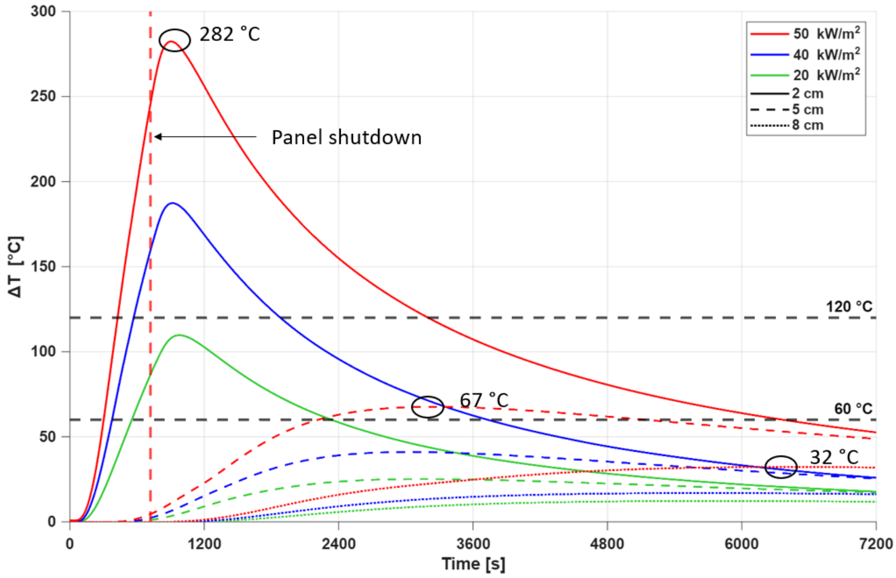

Figure 5: Evolution of ΔT for 20, 40 and 50 kW.m^{-2} at depths of 2, 5 and 8 cm.

The simultaneous representation of the three heat flux densities (20, 40 and 50 kW.m^{-2}) at depths of 2, 5 and 8 cm in Figure 5 highlights the coupled effect of flux intensity and depth. It clearly appears that the higher the imposed heat flux density, the greater the temperature rise. However, increasing depth significantly attenuates this heating, regardless of the applied flux density. When comparing the maximum temperature variation for 50 kW.m^{-2} between 2 and 5 cm, the reduction reaches about 76% and nearly 89% between 2 and 8 cm. This overall comparison thus illustrates the protective role of depth against surface thermal loads and confirms that the severity of the phenomenon decreases markedly with increasing soil depth.

Under the most severe condition (50 kW.m^{-2}), thermal risks become negligible beyond 6 cm and disappear above 10 cm, confirming the strong attenuation capacity of soil and the critical role of the near-surface layer (0–5 cm). It should be emphasized that the studied soil, composed of dry sand, is an inert medium with good insulating properties. Further tests on more representative, possibly reactive natural soils (clayey, loamy, peat and lignite) and/or moist or not, are required to confirm and generalize these observations.

4. Conclusion

This study has provided new insights into the impact of wildland fires on soils and on the buried infrastructures or objects they may contain. Two complementary experimental campaigns were conducted: the first on a burn table, to measure the released heat flux densities and the second in an instrumented tank to analyze heat propagation in depth. The results showed that the critical thresholds identified for buried networks (60 °C) and for munitions (120 °C) can be exceeded within the top five centimeters of soil, particularly under high heat flux exposure (50 kW.m^{-2}). Thus, this work represents a first step toward a better assessment of the risk of degradation of underground networks and the accidental triggering of buried munitions during wildfires. Future perspectives include extending the experiments to more representative soil types (clayey, loamy or peat soils) and accounting for the effect of soil moisture.

Références

[1] INRAE, *Le dérèglement climatique attise les risques de feux de forêt en France*, août 2022.

[2] M. W. Jones, D. I. Kelley, C. A. Burton, S. H. Doerr, A. Arneth, *et al.*, *State of wildfires 2023–2024*, Earth System Science Data, 16(8) (2024) 3601–3623.

[3] X. Silvani, F. Morandini, Fire spread experiments in the field: temperature and heat fluxes measurements, *Fire Safety Journal*, 44(2) (2009) 279–285.

[4] D. Frankman, B. W. Webb, B. W. Butler, D. Jimenez, J. M. Forthofer, *et al.*, Measurements of convective and radiative heating in wildland fires, *International Journal of Wildland Fire*, 22(2) (2012) 157–167.

[5] E. V. Mueller, N. Skowronski, J. C. Thomas, K. Clark, M. R. Gallagher, *et al.*, Local measurements of wildland fire dynamics in a field-scale experiment, *Combustion and Flame*, 194 (2018) 452–463.

[6] M. D. Busse, C. J. Shestak, K. R. Hubbert, Soil heating during burning of forest slash piles and wood piles, *International Journal of Wildland Fire*, 22(6) (2013) 786–796.

[7] E. G. Richter, *Simulation of heat transfer through soil for the investigation of wildfire impacts on buried utilities*, Master's thesis, Oregon State University, 2021.

[8] M. L. Janssens, Predicting Temperature Profiles in Soil and the Effect of Heat Conduction on Buried Thermoplastic Pipes During a Wildfire, *Fire and Materials* (2025).

[9] G. Rein, N. Cleaver, C. Ashton, P. Pironi, J. L. Torero, The severity of smouldering peat fires and damage to the forest soil, *Catena*, 74(3) (2008) 304–309.

[10] A. Lhuillier-Marchand, *Propagation des feux de végétation : expérimentations à l'échelle du laboratoire et validation d'un propagateur*, Thèse de doctorat, Université de Lorraine, 2016. URL: `https://theses.hal.science/tel-01487015`.

[11] M. R. Laverdière, S. Thibaudeau, Pratiques culturales pour conserver le sol, dans *Conservation des sols argileux et sablonneux*, Québec, Canada, 1990, pp. 117–139 (15e Colloque de Génie rural).

[12] R. C. Rothermel, *A mathematical model for predicting fire spread in wildland fuels*, USDA Forest Service, Research Paper INT-115, 1972.